Regional Studies in Marine Science 35 (2020) 101197

Contents lists available at ScienceDirect

Regional Studies in Marine Science

journal homepage: www.elsevier.com/locate/rsma

# An assessment of Brazil Current surface velocity and associated transport near 22°S: XBT and altimetry data

Ivenis I.C. Pita [a,*], Mauro Cirano [a,b], Mauricio M. Mata [c]

[a] Postgraduate Program in Meteorology, Federal University of Rio de Janeiro (UFRJ), Brazil
[b] Institute of Geosciences, Federal University of Rio de Janeiro (UFRJ), Brazil
[c] Institute of Oceanography, Federal University of Rio Grande (FURG), Brazil

ARTICLE INFO

*Article history:*
Received 13 August 2018
Received in revised form 31 October 2019
Accepted 21 February 2020
Available online 27 February 2020

*Keywords:*
Western Boundary Current
Brazil Current
AX97 reference transect
XBT
Altimetry data

ABSTRACT

The use of Expendable Bathythermographs (XBTs) is widespread throughout the world's oceans. 15 XBT high-density transects are located only in the Atlantic Ocean. However, the only transect that exclusively monitors the Brazil Current (BC) is the NOAA/AOML AX97 transect, running from Rio de Janeiro to Trindade Island. The BC is the Western Boundary Current linked to the circulation of the South Atlantic subtropical gyre. Surface velocity field based on the AX97 XBT data reference transect and two different altimetry datasets (AVISO and ATOBA) are compared with the objective of assessing the impact of different horizontal resolution altimetry products on averaged BC dynamical features. Furthermore, a sensibility study is performed considering different approaches to estimate BC volume transports. Data from 43 AX97 cruises, covering the period from Jan/2004 to Dec/2013 were used. AVISO (ATOBA) data are daily (weekly) and present a spatial resolution of 1/4° (1/12°). AX97 geostrophic velocity values were calculated based on XBT data using the isopycnal of $\sigma_\theta = 26.8$ kg/m$^3$ as the reference level of no motion, whereas the altimetry surface geostrophic velocities were obtained based on maps of absolute dynamic topography. About 80.5% (74.4%) of the time, at least one altimetry dataset observed the BC core at AX97 region. ATOBA dataset presented a better performance if compared to AVISO when the BC is highly unstable. Also, in coastal areas, where the flow frequently changes direction, a high-resolution altimetry product (ATOBA) tends to represent the horizontal structure of the BC better than AVISO, where BC horizontal pattern is smoother. Finally, the merge between AX97 data and altimetry datasets presented some inconsistencies when surface currents are in opposite directions. It is recommended to combine AX97 data with another type of data acquired in deeper regions, where near-zero velocities will propagate a smaller error along the water column.


## 1. Introduction

The use of Expendable Bathythermographs (XBTs) for temperature data acquisition is vital for the understanding of the upper ocean. An overall of 18,000–20,000 XBTs are deployed per year around the globe (Bringas and Goni, 2015; Cheng et al., 2016). Most of these launches are performed by local or regional research groups. On the other hand, the coordination and support of international programs are indispensable for successful data acquisition, quality control and application in different studies (Abraham et al., 2013). In the Atlantic Ocean, the XBT Network is a project created by the National Oceanic and Atmospheric Administration/Atlantic Oceanographic and Meteorological Laboratory (NOAA/AOML) and oversight by Ship-Of-Opportunity Program Implementation Panel. NOAA/AOML XBT Network coordinates 15 high-density transects on the Atlantic Ocean. A high-density transect is characterized by XBT deployments every 10–15 nm and realization of approximately four times per year (Cheng et al., 2016). NOAA/AOML XBT Network data are used in a series of studies regarding ocean surface currents (e.g. Goes et al., 2013a), meridional heat transport (e.g. Garzoli and Baringer, 2007) and Atlantic Meridional Overturning Circulation (AMOC) (e.g. Dong et al., 2009, 2015; Goes et al., 2015a,b). Due to the importance of XBT data on oceanographic studies, several studies focused on the understanding of their uncertainties, such as inferred depth based on Fall Rate Equation (FRE) and XBT temperature biases (e.g. Reverdin et al., 2009; DiNezio and Goni, 2010, 2011; Goes et al., 2013b; Hutchinson et al., 2013; Bringas and Goni, 2015; Ribeiro et al., 2018). In addition, Cheng et al. (2016) compared 10 available correction schemes that consider global and historical XBT datasets and considered the correction scheme proposed by Cheng et al. (2014) as the most appropriated for XBT data. However, Cheng et al. (2016) also stated that XBT data with no

* Corresponding author.
*E-mail address:* ivenis.pita@rsmas.miami.edu (I.I.C. Pita).

https://doi.org/10.1016/j.rsma.2020.101197
2352-4855/

correction scheme can provide a good estimate for geostrophic current. Finally, Goes et al. (2015a) analyzed the impact of XBT biases on AMOC estimations and found that XBT biases after 2010 could result on errors of up to 3% (0.38 Sv) on the AMOC.

The use of XBT is widespread throughout the world's oceans. From the 15 XBT high-density transects located in the Atlantic Ocean, almost one third is fully or partially positioned in the Southern Hemisphere. The main dynamic feature of the South Atlantic Ocean is the South Atlantic subtropical gyre. The South Atlantic Current, the Benguela Current, the South Equatorial Current (SEC) and the Brazil Current (BC), that completes the gyre, compose the subtropical gyre. The BC, a Western Boundary Current (WBC), is originated at the bifurcation of SEC, however, additional flow inputs are observed at different depths and latitudes (Stramma and England, 1999). Pereira et al. (2014) performed a series of model runs and detailed the SEC bifurcation process for the three main water masses: between 13° and 15°S for the level of the Tropical Water (TW); about 22°S for the South Atlantic Central Water (SACW) level, and between 28° and 30°S at the Antarctic Intermediate Water level. On the other hand, Calado et al. (2008) stated that the SACW bifurcation was north of 22°S and also that the BC transports TW and SACW between 20 and 28°S. Finally, the only NOAA/AOML XBT Network transect that exclusively monitors the BC is the AX97 (Fig. 1).

Between 18°S and 24°S, the BC pattern is strongly influenced by regional bathymetry and mesoscale features (e.g. Schmid et al., 1995; Stramma and England, 1999; Soutelino et al., 2011; Mill et al., 2015). Abrupt changes in flow direction are frequently observed around 22°S. Eddies and meanders are the main sources of variability of BC flow (Campos et al., 1995; Campos, 2006; Soutelino et al., 2011). Lima et al. (2016) compared the BC baroclinic velocity ($-0.17 \pm 0.30$ m/s) and transport ($-2.7 \pm 3.6$ Sv) with previous studies (e.g. Campos et al., 1995; da Silveira et al., 2008; Mata et al., 2012; Rocha et al., 2014) and confirmed the development of eddies and meanders at 22°S. The meandering pattern of BC corroborates for the development of eddies near 22°S. As a consequence, several authors observed the occurrence of opposite velocities on the shelf break region (e.g. Campos et al., 1995; da Silveira et al., 2004, 2008; Rocha et al., 2014). The intense variability of BC is linked to weather condition at the vicinity of AX97 transect (Mill et al., 2015).

Centered at 20°S, the Vitória-Trindade Ridge (VTR) is the main physical obstacle for the BC along the Brazilian coast (Fig. 1). VTR is a sequence of seamounts displaced zonally at 20°S from the shelf break to the meridian of 29°W. The contrast of depth up to 2000 m and seamounts that can reach tens of meters from the ocean surface creates a complex environment for the continuation of the flow of TW and SACW (Fu, 1981; Evans et al., 1983; Evans and Signorini, 1985). A schematic representation of BC main path and water masses is presented in Calado et al. (2008). In order to pass these obstacles, BC divides its flow along the different channels among the seamounts. Evans et al. (1983) used hydrographic data to describe the BC flow between 19°S and 22°S, where the main flow, located between Besnard Bank and Vitória Seamount (Fig. 1), was responsible for a transport of 3.8 Sv up to 500 m with velocities up to 0.50 m/s. Afterward, the bifurcated current is then, reorganized due to the conservation of potential vorticity into a unique branch close to the continental slope (Evans et al., 1983; Legeais et al., 2013). This mechanism is also responsible for the development of eddies and meanders south of 20°S (Mascarenhas et al., 1971; Signorini, 1978; Schmid et al., 1995; da Silveira et al., 2008; Mill et al., 2015). Some of these eddies are able to translate northward and cross the VTR (Arruda et al., 2013). In addition, frequent anticyclonic eddies are also observed north of the VTR (Soutelino et al., 2011).

Most of the regional studies focused on BC at the vicinity of AX97 transect use hydrographic data on its analysis (Signorini, 1978; Evans et al., 1983; Campos et al., 1995; Müller et al., 1998; da Silveira et al., 2008; van Caspel et al., 2010; Soutelino et al., 2011; Mata et al., 2012; Biló et al., 2014; Palóczy et al., 2014; Rocha et al., 2014; Mill et al., 2015; Lima et al., 2016). Therefore, the reference level adopted is a crucial step for the work and one of the main uncertainties. Even though the studies mentioned above have been based on different reference levels, they converge to the fact that most of the transport of BC is confined in the upper 200 m of the water column.

**Table 1**
MOVAR data acquisition cruises realized from 2004 to 2013 along the AX97 transect. Start and end date (DD/MM/YYYY) are shown for each cruise, as well as the duration in days.
*Source:* Modified from Lima et al. (2016).

| Cruise | Start | End | Duration (days) | Season |
|---|---|---|---|---|
| 1 | 29/08/2004 | 02/09/2004 | 5 | Winter |
| 2 | 17/02/2005 | 20/02/2005 | 4 | Summer |
| 3 | 12/08/2005 | 15/08/2005 | 4 | Winter |
| 4 | 14/02/2006 | 16/02/2006 | 3 | Summer |
| 5 | 30/06/2006 | 02/07/2006 | 3 | Winter |
| 6 | 16/08/2006 | 18/08/2006 | 3 | Winter |
| 7 | 11/12/2006 | 14/12/2006 | 4 | Spring |
| 8 | 25/02/2007 | 28/02/2007 | 4 | Summer |
| 9 | 05/03/2007 | 07/03/2007 | 3 | Summer |
| 10 | 21/04/2007 | 24/04/2007 | 4 | Autumn |
| 11 | 27/06/2007 | 29/06/2007 | 3 | Winter |
| 12 | 24/08/2007 | 30/08/2007 | 7 | Winter |
| 13 | 14/02/2008 | 16/02/2008 | 3 | Summer |
| 14 | 17/04/2008 | 19/04/2008 | 3 | Autumn |
| 15 | 11/06/2008 | 13/06/2008 | 3 | Autumn |
| 16 | 19/08/2008 | 21/08/2008 | 3 | Winter |
| 17 | 06/12/2008 | 08/12/2008 | 3 | Spring |
| 18 | 03/02/2009 | 06/02/2009 | 4 | Summer |
| 19 | 10/04/2009 | 13/04/2009 | 4 | Autumn |
| 20 | 21/06/2009 | 23/06/2009 | 3 | Autumn |
| 21 | 14/10/2009 | 16/10/2009 | 3 | Spring |
| 22 | 09/12/2009 | 11/12/2009 | 3 | Spring |
| 23 | 04/05/2010 | 08/05/2010 | 5 | Autumn |
| 24 | 02/12/2010 | 05/12/2010 | 4 | Spring |
| 25 | 08/02/2011 | 10/02/2011 | 3 | Summer |
| 26 | 03/05/2011 | 06/05/2011 | 4 | Autumn |
| 27 | 13/06/2011 | 15/06/2011 | 3 | Autumn |
| 28 | 16/08/2011 | 23/08/2011 | 8 | Winter |
| 29 | 18/10/2011 | 21/10/2011 | 4 | Spring |
| 30 | 29/11/2011 | 05/12/2011 | 7 | Spring |
| 31 | 24/02/2012 | 27/02/2012 | 4 | Summer |
| 32 | 02/04/2012 | 04/04/2012 | 3 | Autumn |
| 33 | 07/06/2012 | 10/06/2012 | 4 | Autumn |
| 34 | 26/07/2012 | 01/08/2012 | 7 | Winter |
| 35 | 15/08/2012 | 18/08/2012 | 4 | Winter |
| 36 | 22/10/2012 | 01/11/2012 | 11 | Spring |
| 37 | 05/12/2012 | 07/12/2012 | 3 | Spring |
| 38 | 15/02/2013 | 17/02/2013 | 3 | Summer |
| 39 | 13/04/2013 | 17/04/2013 | 5 | Autumn |
| 40 | 24/06/2013 | 28/06/2013 | 5 | Winter |
| 41 | 17/08/2013 | 19/08/2013 | 3 | Winter |
| 42 | 16/10/2013 | 19/10/2013 | 4 | Spring |
| 43 | 30/11/2013 | 03/12/2013 | 4 | Spring |

Satellites are useful tools for the understanding of ocean currents, however, the analysis of WBC dynamics could be challenging for altimetry because the main flow could deviate from isobath-parallel flow toward coastal, and shallower, areas. Coastal areas provide a great source of error for altimetry products. The proximity with land generates problems related with correction of tides, high-frequency atmospheric signal and wet tropospheric components (Dufau et al., 2011).

The main goal of the present study is to assess the performance of two altimetry datasets with different spatial resolutions on capturing the horizontal structure of BC along the AX97 transect, against observations from the NOAA/AOML XBT Network. In order to reach this objective, two secondary goals are addressed: (i) an analysis of the BC core location along the coastal and

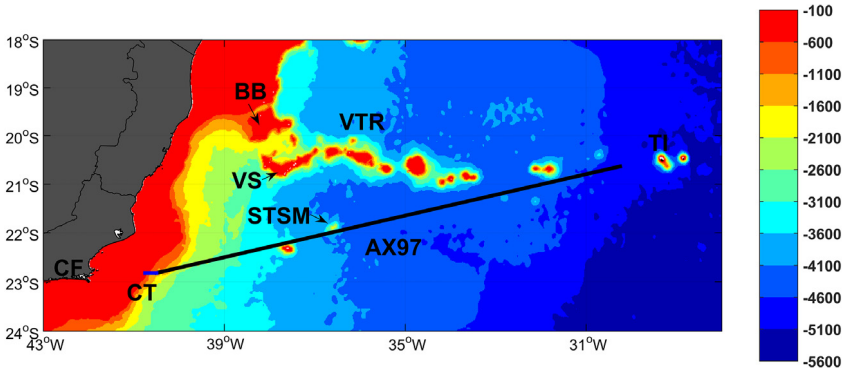


**Fig. 1.** Study site. Colorbar represents local bathymetry in meters. Cabo Frio, Trindade Island, Besnard Bank and Vitória Seamounts are presented by CF, TI, BB, and VS, respectively. Vitoria-Trindade Ridge (VTR) and São Tomé Seamount (STSM) locations are indicated. Blackline represents the AX97 reference transect and the blue line is the coastal transect (CT). (For interpretation of the references to color in this figure legend, the reader is referred to the web version of this article.)

the AX97 transects and (ii) the discussion of the (dis)agreement between different altimetric products and velocity field based on XBT measurements. In addition, a sensitivity study will be performed considering the same volume transport approach for different velocity fields.

## 2. Material and methods

This study is based on XBT data and two altimetry datasets. Since XBT data are not acquired continuously in time, from now on the continuous period between Jan/2004 and Dec/2013 is referred as the "Total Period" (TP) whereas the period of XBT data acquisition is referred as the "Cruise Period" (CP) (see Table 1).

### 2.1. AX97 data

Temperature data was collected in the framework of project MOVAR (Monitoring the upper ocean transport variability in the western South Atlantic) through XBT deployments between Cabo Frio – RJ (CF) and Trindade Island (TI) (Fig. 1). XBT sampling was performed with a horizontal resolution of 27 km along AX97 transect and 18 km at both endings of the transect. Most of the XBT probes used were Sippican Deep Blue probes, which reach depths of up to 800 m. In addition, Sippican T-5 probes, which measure temperature profiles down to 1830 m, were deployed in a lower frequency scheme. The salinity profile was estimated by a polynomial temperature function, based on the historical relations of Temperature–Salinity (Thacker, 2007; Thacker and Sindlinger, 2007; van Caspel et al., 2010). More specifically, the methodology developed by van Caspel et al. (2010) was used, which was developed specially for the surrounding areas of VTR. Afterward, data are interpolated onto the AX97 reference transect, which has a horizontal spatial resolution of 1/4°, and 10 m depth for each cell, following the method described by Lima et al. (2016). AX97 data are freely distributed by AOML (http://www.aoml.noaa.gov/phod/hdenxbt/ax_home.php?ax=97), and supported by NOAA/AOML XBT Network. Between 2004 and 2013, 43 oceanographic cruises with an average duration of 4 days were performed on the AX97 transect, with an average frequency of 4 to 5 cruises per year. Table 1 presents some details of each cruise.

The dynamical method was used in order to obtain the baroclinic geostrophic velocity (Pond and Pickard, 1983). The $\sigma_\theta = 26.8$ kg/m$^3$ isopycnal was used as the reference level of no motion for the calculation of the geostrophic velocity, once this density value is largely accepted as the interface between the BC and the Intermediate West Boundary Current (Biló et al., 2014; Pereira et al., 2014). The use of an isopycnal reference for AX97 data is determinant for a good representation of the mean flow across the referred transect. Finally, the cross-section volume transport was estimated based on a vertical integration of the velocity field, for the AX97 transect, from the surface to the depth of the isopycnal $\sigma_\theta = 26.8$ kg/m$^3$ (Mata et al., 2012).

The inaccuracies in methodologies applied in ocean currents studies with XBT data are centered on four main points: (i) FRE uncertainties; (ii) temperature bias; (iii) inferred salinity, and (iv) the definition of the reference level. In order to diminish intrinsic equipment error, a correction was performed on FRE and temperature bias following the most applied methodology described by Cheng et al. (2014), even though no correction scheme was needed for geostrophic current studies (Cheng et al., 2016). The scheme proposed by Cheng et al. (2014) was chosen in order to use the most recommended correction scheme regardless the XBT data application. Root mean square salinity errors close to 0.15 psu and 0.35 psu at 25 dbar were estimated for Gulf Current and the Sargasso Sea, respectively. Errors with an order of magnitude smaller were estimated below at the thermocline region (Thacker, 2007; Thacker and Sindlinger, 2007). The use of different methods on inferring the salinity field could result in differences on volume transport between 0.5 and 2.0 Sv for South Java Current (Sprintall et al., 2002). For the VTR, van Caspel et al. (2010) found volume transport errors up to 0.8 Sv.

Regarding the reference level adopted for BC transport estimates, various studies were performed based on different levels (Table 2). Long-period analysis carried out by Mata et al. (2012) and Lima et al. (2016) present a difference of mean volume transport for BC at 22°S close to 15%. Several authors from all over the world target an optimal reference level. For instance, Sprintall et al. (2002) observed a mean difference of almost 30% on volume transport on Indonesian Throughflow only because of the reference level definition.

In order to apply the geostrophic flow and thermal wind approaches, one of the assumptions made is the existence of a frictionless flow (Pond and Pickard, 1983). In addition, WBCs tent to flow along the continental slope and nevertheless different processes could deviate the flow across the shelf break (wind stress, bottom influence, cascading, meanders and eddies), resulting in a WBC flowing at shallow regions ($<$200 m). Therefore, the proximity with the coast is one of the main limiting factors for the use of dynamical method on the analysis of WBC dynamics (Simpson and Sharples, 2012).

### 2.2. Altimetry data

A total of two altimetry datasets were used on this work. Surface geostrophic velocity data (between 18–24°S and 28–43°W)

**Table 2**
Brazil current volume transport estimates between 20° and 25° S. The last column indicates the reference level (RL) adopted.

| Latitude | Transport (Sv) | Work | RL |
|---|---|---|---|
| 20.28 S | −3.8 | Evans et al. (1983) | 500 m |
| 20.3 S | −1.6 | Stramma et al. (1990) | 590–630 m |
| 21 S | −9.4 | Schmid et al. (1995) | 600 m |
| 21.4 S | −4.4 | Evans et al. (1983) | 500 m |
| 22 S | −3.0 | Pereira et al. (2014) | 300 m |
| 22 S | −5.2 | Signorini (1978) | 500 m |
| 22 S | −5.5 | Lima (1997) | Current meter |
| 22.5 S | −2.3 | Mata et al. (2012) | 400 m |
| 22.5 S | −2.7 | Lima et al. (2016) | Isopycnal ($\sigma_\theta = 26.8$ kg/m$^3$) |
| 22–25 S | −4.8 | da Silveira et al. (2008) | Current meter |

**Table 3**
Location of the BC core and its frequency of occurrence based on the total period (cruise period) analysis. "AX97" column represents events where both altimetry data captured the BC core along the AX97 transect. "CT" column counts the weeks (cruises) where BC's core was observed at the coastal transect by both altimetry data. The last column indicates the events where only one of the altimetry data captured the BC core along AX97 transect.

| | AX97 | CT | AX97/CT |
|---|---|---|---|
| Weeks (cruises) | 314 (21) | 101 (11) | 106 (11) |
| Frequency (%) | 60.3 (48.8) | 19.4 (25.6) | 20.3 (25.6) |

were obtained from the AVISO (Archiving, Validation, and Interpretation of Satellite Oceanographic) delayed time product provided by Ssalto Multimission Ground Segment/Data Unification and Altimeter Combination System (SSALTO/DUAC). These data were available on daily maps of absolute dynamic topography, with a spatial resolution of 1/4° (CLS, 2015a).

ATOBA (Altimetry Tailored and Optimized for Brazilian Applications) dataset were obtained from the delayed time product of the V2 region (between 11–34°S and 32–54°W) provided by the Oceanographic Modeling and Observation Network (REMO) and by the system SSALTO/DUAC (CLS, 2015b). ATOBA products consider a series of coastal altimetry corrections (e.g. ionospheric correction, dry and wet troposphere corrections, ocean tide, orbit error, longwave errors, sea state bias). All coastal altimetry corrections considered on ATOBA dataset are listed by CLS (2015b). Among them, it is worth to mention (i) the Sea State bias, which is one of the most important correction for coastal altimetry products and is related to a reduced altimetry accuracy because of ocean waves (Chelton et al., 2001). For ATOBA V2 product, a non parametric sea state bias was used. In addition, (ii) orbit errors were diminished with the help of global multi-mission crossover minimization; (iii) optimal interpolation was used in order to decrease longwave errors and (iv) the Topex microwave radiometer was used to implement the tropospheric corrections. ATOBA V2 also presents improvements on along-track resolution and tide corrections made by FES-2012 model if compared to other versions of the same product (Daher and Junior, 2014). Furthermore, small and medium noise were eliminated from along-track data by improved atmospheric and geophysical corrections (Daher and Junior, 2014). Moreover, the outputs are disposed on a 1/12° horizontal grid.

Weekly Sea Surface Height Anomaly (SSHA) maps were provided by ATOBA, and the Mean Dynamic Topography (MDT) was calculated based on historical data of 20 years. The surface geostrophic velocity was calculated based on Eqs. (1)–(3) (Benny et al., 2015). The components of the geostrophic velocity anomaly ($u'$ and $v'$) were estimated from SSHA (Eqs. (1) and (2)) where:$g$ is the gravity force; $f$ is the Coriolis parameter; $\delta x$ and $\delta$y are the zonal and meridional distance between the points, respectively; and $\delta h$ is the difference of the SSHA between consecutive points.

$$u' = \frac{-g}{f} \cdot \frac{\delta h}{\delta \mathrm{y}} \tag{1}$$

$$v' = \frac{g}{f} \cdot \frac{\delta h}{\delta x} \tag{2}$$

The mean geostrophic velocity ($Vmg$), obtained from the MDT, combined to the geostrophic velocity anomaly ($Vg'$), obtained from the SSHA, result in the total geostrophic velocity ($Vg$) as follows

$$Vg\,(x, y, t) = Vmg(x, y) + Vg'(x, y, t) \tag{3}$$

Surface velocity data from AVISO and ATOBA were interpolated and rotated (approximately 13.025° counterclockwise) to the points of the AX97 reference transect. A coastal transect (CT) was also created in order to connect the coast of Cabo Frio (RJ) with the western limit of AX97 transect (Fig. 2). Only stations deeper than 200 m were considered. This transect presents the same spatial resolution of AX97. All stations with a depth shallower than 200 m were not considered on the analyses. Bathymetry data obtained by GEBCO 2014 was used.

### 2.3. XBT/altimetry data coupling

In order to perform a sensitivity experiment, XBT based geostrophic velocity fields were combined with altimetry datasets to obtain the subsurface baroclinic velocity field. The subsurface velocity structure from the thermal wind equation (Eqs. (4) and (5)) was re-referenced on the surface with the geostrophic velocity provided by AVISO and ATOBA. For comparative purposes, the subsurface geostrophic fields will be obtained up to the isopycnal depth of $\sigma_\theta = 26.8$ kg/m$^3$.

$$\frac{\delta \mathrm{u}}{\delta \mathrm{z}} = \frac{\mathrm{g}}{\rho f} \cdot \frac{\delta \rho}{\delta \mathrm{y}} \tag{4}$$

$$\frac{\delta \mathrm{v}}{\delta \mathrm{z}} = -\frac{\mathrm{g}}{\rho f} \cdot \frac{\delta \rho}{\delta \mathrm{x}} \tag{5}$$

where u and v are the zonal and meridional geostrophic velocity components, respectively; $\rho$ is the water density, and $x$, y and z are the spatial coordinates.

As ATOBA data presents a weekly frequency, the mean velocity of each cruise was calculated based on a weighted average. The weight of each weekly data was directly related to the number of days the cruise operated during the week. For example, if a cruise gathered data for 5 days (from Friday to Tuesday), the representative velocity for the entire cruise for each station would be:

$$\frac{(n1 \times Vweek1) + (n2 \times Vweek2)}{duration\ of\ the\ cruise\ (days)} \tag{6}$$

where, $n1$ ($n2$) is the total of days of the 1st (2nd) week which there was data acquisition and $Vweek1$ ($Vweek2$) is the weekly velocity component obtained from the ATOBA product. In the case of the example above, the coefficient $n1$ ($n2$) would be equal to 2 (3) and the duration of the cruise would be 5 days.

The mean velocity of each cruise for the AVISO data was calculated based on the mean daily velocity corresponding to

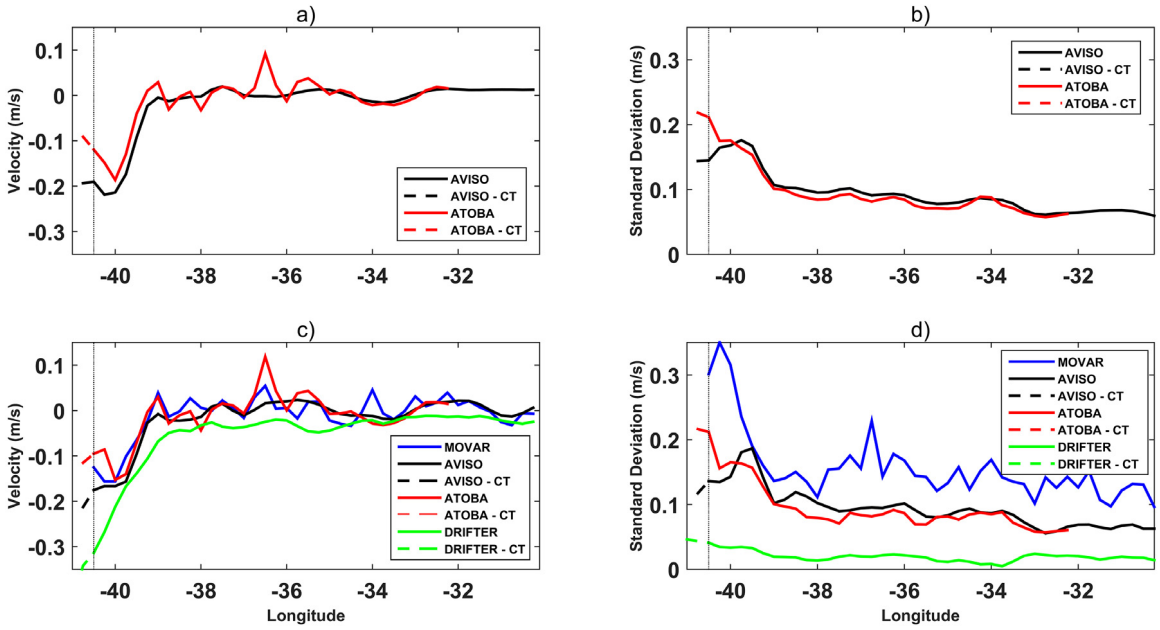


**Fig. 2.** Cross component of surface velocity for coastal and AX97 transects. a- and b- are the mean surface velocity and associated variability for the total period, where only the altimetry data is presented. The same is expressed in c- and d- for the cruise periods. Solid (dashed) line represents AX97 (Coastal transect). The acronyms MOVAR, ATOBA, AVISO and DRIFTER are used to indicate data associated with XBT, altimetry and drifters, respectively. Geographical location of transects is presented in Fig. 1. Negative values indicate a southward flow. (For interpretation of the references to color in this figure legend, the reader is referred to the web version of this article.)

the period of each cruise (Table 1). Surface velocities were also grouped by season for both TP and CP.

The resultant volume transport was obtained by vertical integration (from the surface to the depth of isopycnal $\sigma_\theta = 26.8$ kg/m$^3$) of the geostrophic velocity profile along the AX97 reference transect. In addition, the BC volume transport was considered as the along transect integration of the volume transport from the westernmost section of AX97 transect up to 39°W. This process was performed for both TP and CP.

### 2.4. Data analysis

All datasets were subdivided into CP, while only the altimetry datasets had the TP established. It was not possible to include the TP analysis for AX97 data because data acquisition is not continuous.

In order to analyze the longitudinal extension of the BC, the mean and standard deviation of the surface velocity of each cruise for AX97 data and altimetry datasets were considered. The standard deviation is used as a proxy of current's variability. The BC core was defined as the point where the southward flow presents the highest intensity between the shelf break and 39°W. Even though, some studies have shown that the BC core is located on the subsurface (∼100 m depth) (Lima et al., 2016), the surface velocity fields based on both altimetry and XBT data were used to establish the BC core location because the coupling between XBT and altimetry datasets was used as a sensitivity study.

The cruises were subdivided into 3 main groups regarding the BC core location from altimetry datasets: (i) the core is found along the AX97 reference transect in both altimetry datasets; (ii) the core is positioned along the AX97 reference transect for only one altimetry product and (iii) the BC core is located onshore of the AX97 reference transect in both datasets. Finally, the resultant volume transport was calculated for altimetry datasets using the coupling methodology mentioned previously and study cases for cruises #7 and #20 were performed, because their results were contrasting in terms of the coupling methodology applied.

## 3. Results and discussion

### 3.1. Surface velocity

The mean surface velocity for the TP and the associated standard deviation for AX97 and altimetry datasets analyzed are shown in Fig. 2. BC is represented by its mean southward flow and large variability from 40.5°W up to 39°W. Therefore, this manuscript considers the BC as the flow across AX97 transect between its westernmost point and 39°W. The latest was chosen because it is the longitude where the standard deviation decreases sharply in comparison with westernmost longitudes, indicating a less frequent influence of BC highly variable system. In addition, the variability pattern on the eastward direction remains with a similar/smooth pattern. Furthermore, BC system is extremely variable, where its variability can reach values equal to or higher than the mean flow. Another important aspect is the difference of spatial resolution between AVISO and ATOBA. For example, in Figs. 2.a and 2.c, whilst ATOBA (spatial resolution of 1/12°) captures the information of the northward flux close to São Tomé Sea Mount (STSM) (36.5°W), AVISO (spatial resolution of 1/4°) hardly recognizes its signal. Fig. 2 provides useful information regarding the applicability of this research, both in terms of the representativity of the area analyzed and also regarding the influence of high-resolution altimetry data (e.g. ATOBA). In addition, Drifter-derived Monthly Climatology of Global Near-surface Currents (Laurindo et al., 2017) was used as an independent measurement. After interpolating and rotating both drifter-based velocity components to the CT and AX97 transect, the mean and the standard deviation was plotted in order to compare the drifter-derived BC surface velocity to XBT-based and altimetry datasets (Figs. 2.c and 2.d). The mean drifter-based BC section was similar to all products analyzed, however the variability of the drift-based climatology presented significantly lower values than other products. This occurred because the standard deviation was based on a monthly climatology.

Table 3 details the position of the BC core and how frequently the core is observed along the AX97 reference transect. Considering the TP (CP), in 60.3% (48.8%) of the weeks (cruises), both altimetry datasets identify BC core within AX97 transect. Furthermore, in 80.5% (74.4%) of the time, at least one altimetry dataset observes the BC core at AX97 region. The similarity of the mean flow from altimetry data between TP and CP (Figs. 2.a and 2.c) with AX97 data and the information from Table 3 confirms that all data analyzed in this study are robust and indicates that MOVAR samples the thermal structure with enough spatial and temporal resolution to achieve representative mean results.

A more detailed analysis of the three scenarios identified in Table 3 is presented in Figs. 3–5. When the BC core is located at AX97 reference transect on both altimetric products (Fig. 3), the maximum southward flow tends to be between 40.25°W and 40°W. In this scenario, the BC core achieved mean values of $-0.32 \pm 0.38$ m/s (ATOBA), $-0.24 \pm 0.18$ m/s (ATOBA) and $-0.26 \pm 0.12$ m/s (AVISO), respectively. A transitional stage is observed in Fig. 4, where only one altimetry dataset identified the BC core inside the AX97 region. In this case, two zones with maximum southward flow are observed. The first one is located around 39.7°W and the second region is located at the western point analyzed (40.5°W and 40.75°W for AX97 and altimetry data, respectively). However, two or more peaks of negative flow could not necessarily be exclusively related to bifurcation processes, since meanders events are also represented by this pattern observed in Figs. 4.a and 5.a (for AX97 and ATOBA data). This scenario presented the most elevated variability, which was expected once it deals with a transition between two contrasting patterns. Furthermore, in coastal areas, ATOBA tends to represent the horizontal structure of the BC better than AVISO, once the original higher-resolution altimetry product can perceive the highly variable BC flow better than AVISO and had an important impact on perceiving the BC core in coastal areas. It is important to mention that coastal altimetry corrections of ATOBA data are partially responsible for a better representation (when compared to AVISO) of BC variability on the western portion of AX97 transect with reference to the MOVAR data (Fig. 2.d).

Events where both altimetry datasets capture the BC core within the CT are observed on Fig. 5. The most intense velocities are observed on the CT for AVISO ($-0.34 \pm 0.09$ m/s) and ATOBA ($-0.31 \pm 0.09$ m/s) data, and on the westernmost point of AX97 transect for AX97 data ($-0.13 \pm 0.23$ m/s). Therefore, in this scenario, altimetry data was decisive for a better understanding of the BC structure. It is important to mention that the western maximum southward flow observed in Figs. 4.a and 5.a does not represent precisely the BC core. A WBC tends to flow along the shelf break according to Taylor–Proudman theorem (Simpson and Sharples, 2012). However, several studies around the world described events where WBCs deviate from isobath-parallel flow, reaching the adjacent continental shelf (e.g. Lutjeharms et al., 1989; Huthnance, 1995; Harris et al., 1996; Savidge and Bane, 2001; Schaeffer et al., 2014; Ding et al., 2016). These events are challenging for XBT and altimetry data for various reasons. In shallower areas, XBT data are not efficient in obtaining the velocity of a current because the geostrophic balance is unattained due to elevated boundary shear values. In addition, altimetry products in the recent past presented elevated errors in areas shallower than 200 m as a consequence of the land contamination in the footprint and due to problems related with correction of tides, high-frequency atmospheric signal and wet tropospheric components (Dufau et al., 2011). While significant improvements have been achieved in the past years (e.g. Roblou et al., 2011; Passaro et al., 2014, 2018; Birol et al., 2017; García et al., 2018), recent developed corrections were not applied on ATOBA methodology.

The higher variability presented by AX97 data (Figs. 2.d, 3.b, 4.b, and 5.b) was expected to occur once the BC system is highly variable (Schmid et al., 1995; Stramma and England, 1999; Mill et al., 2015; Lima et al., 2016). However, it is important to mention that part of this elevated variability could be related to uncertainties inherent to the methodology applied, such as instrument failure, errors due to FRE inaccuracies, local currents, errors related to inferred salinity and so forth. Moreover, the energy filtered by the altimetry datasets are not filtered by AX97 data due to its higher spatial frequency sampling. AVISO data captures only features higher than 1/4°, while ATOBA can identify processes down to 1/12°.

**Table 4**
Cross-correlation for altimetry and AX97 datasets at the AX97 transect for different seasons and cruise period.

| | AVISO | ATOBA |
|---|---|---|
| Summer | 0.43 | 0.41 |
| Fall | 0.51 | 0.49 |
| Winter | 0.44 | 0.40 |
| Spring | 0.42 | 0.45 |
| CP | 0.46 | 0.45 |

**Table 5**
Number of events divided throughout the seasons. "AX97" row represents events where both altimetry data diagnosed the BC core along the AX97 transect. "CT" row counts the cruise periods where the BC's core was observed at coastal transect by both altimetry data. "AX97/CT" row indicates the events where only one of the altimetry data captured the BC core along the AX97 transect. The last row sums the total of cruises realized in each season.

| | Summer | Fall | Winter | Spring |
|---|---|---|---|---|
| AX97 | 6 | 5 | 6 | 4 |
| CT | 3 | 2 | 2 | 4 |
| AX97/CT | – | 3 | 5 | 3 |
| Total | 9 | 10 | 13 | 11 |

Cross-correlation between altimetry and AX97 data were performed for CP and seasonal periods (Table 4). AVISO and ATOBA presented similar cross-correlations with AX97 dataset considering the CP (0.46 and 0.45, respectively). As this cross-correlations analyze a transect with more than 600 nm, these values are acceptable. When these cross-correlations are analyzed considering the different seasons, AVISO presented a slightly higher correlation than ATOBA. Nevertheless, a remarkable fact observed in Table 4 is the seasonality influence in the AX97 correlation. The only period where ATOBA presented a correlation higher than AVISO is during spring. A cross-correlation of 0.42 and 0.45 during spring cruises (AVISO and ATOBA, respectively) is explained by the occurrence at the same rate of all 3 scenarios analyzed previously (Table 5). Furthermore, ATOBA dataset presented a better performance when the BC is highly unstable (spring season). In other words, a greater diversity of events is expected to happen during spring months, leading to enhanced variability.

The relation between velocities obtained by AX97 and altimetry datasets is expressed in Fig. 6. Positive values indicate that altimetry data underestimates the southward flow when compared to the XBT based data. In general, when analyzing areas with absolute surface flow higher than 0.05 m/s, AVISO product, tends to overestimate XBT based surface velocities along AX97 transect in 22%, while the later tends to be underestimated by ATOBA surface velocities in only 3% (not shown). The same analysis for all referenced stations along AX97 transect is impracticable because the relative difference between altimetry and AX97 velocities reach values up to 2000%, once absolute velocities are closed to zero. An intense standard deviation in the region influenced by the BC, as expected, was presented (Fig. 6). A slight decrease of the variability of the mean difference between ATOBA and AX97 data on the area of influence of BC, when

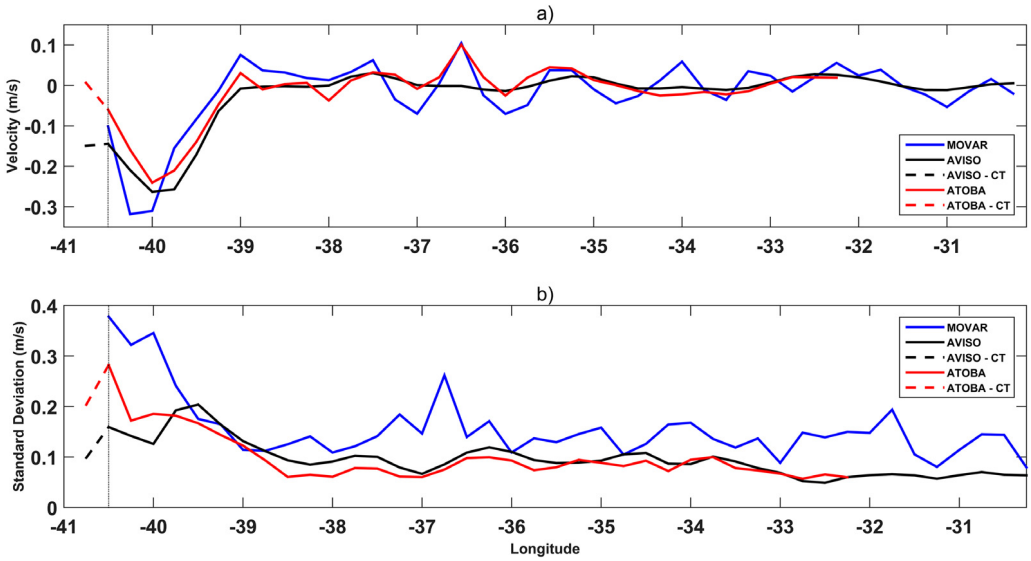


**Fig. 3.** Cross component of surface velocity for coastal and AX97 transects. a- and b- are mean surface velocity and associated variability for events where the BC core was identified at the AX97 for both altimetry datasets. Solid (dashed) line represents AX97 (Coastal transect). Geographical location of transects is presented in Fig. 1. Negative values indicate a southward flow.

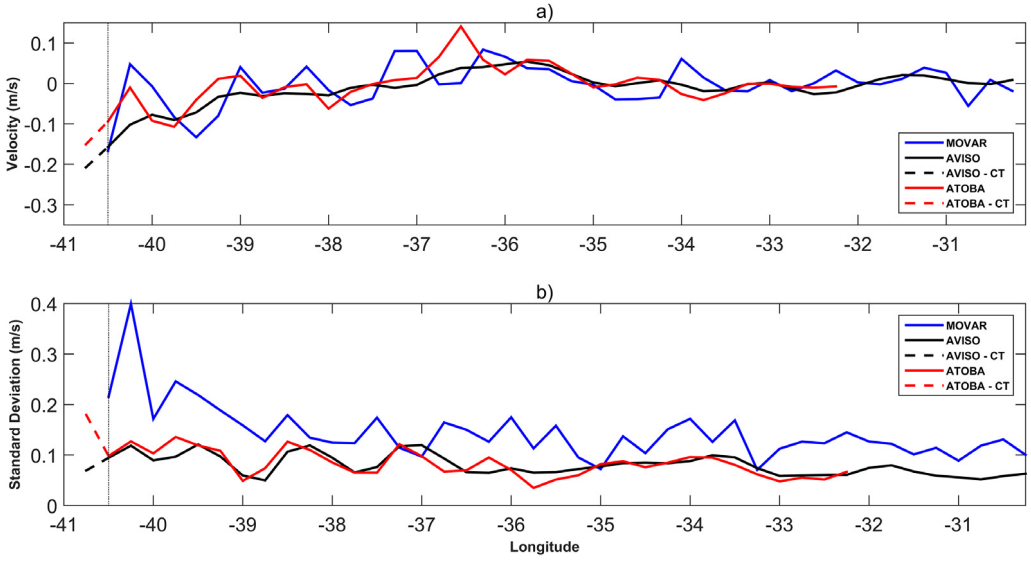


**Fig. 4.** Cross component of surface velocity for coastal and AX97 transects. a- and b- are mean surface velocity and associated variability for events where the BC core was identified at the AX97 in only one altimetry dataset. Solid (dashed) line represents AX97 (Coastal transect). Geographical location of transects is presented in Fig. 1. Negative values indicate a southward flow.

compared to AVISO, confirms the better performance of high-resolution altimetry product in capturing the surface BC flow. In other words, the use of ATOBA product represents a gain of 3.4% on BC dynamical assessment when compared to AVISO dataset, considering ATOBA slightly lower variability on the difference between ATOBA and MOVAR datasets (Fig. 6.b).

The frequency of occurrence when altimetry and AX97 datasets result in opposite direction vectors is expressed in Fig. 7. In 42% (43%) of the points analyzed, AVISO (ATOBA) presented surface velocity vectors pointed for the opposite direction when compared to AX97. The same analysis for the western portion of AX97 transect (40.5° to 39°W) shows a slight improvement for both datasets (41% and 40% for AVISO and ATOBA, respectively). In other words, when considering the BC area of influence, ATOBA was slightly more frequently describing a flow on the same direction of AX97 data. This result corroborates with the previous paragraph statements that ATOBA dataset better assess dynamically the BC if compared to AVISO. However, as the occurrence of opposite flows (between altimetry and AX97 data) can be considered elevated (>40%), this result suggests: (i) that different spatial and temporal resolutions of altimetry and AX97 data may play an important role in observing a flow with opposite direction and, (ii) improvements on AX97 data are still possible to be made (e.g. enhances on determining the reference level for geostrophic velocity calculus or increasing spatial coverage and temporal resolution).

### 3.2. Integrated transport

As AX97 data are underestimated by ATOBA product in only 3%, a good agreement between AX97 and ATOBA resultant transport should be expected, mainly when compared to AVISO. However, when analyzing the cumulative volume along the AX97 transect (Fig. 8), the BC mean resultant transport is estimated in

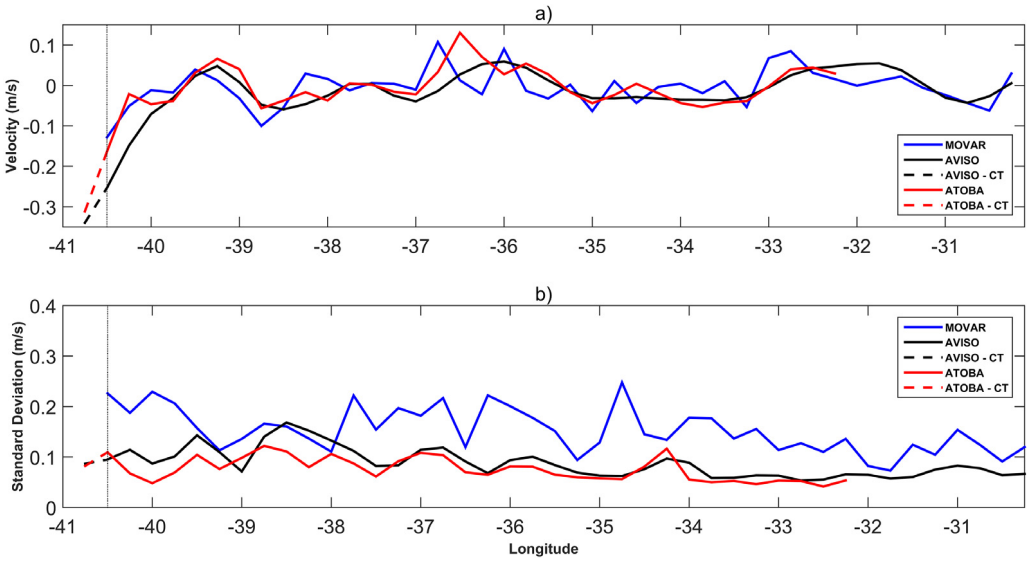


**Fig. 5.** Cross component of surface velocity for coastal and AX97 transects. a- and b- are mean surface velocity and associated variability for events where the BC core was identified at the CT for both altimetry datasets. Solid (dashed) line represents AX97 (Coastal transect). Geographical location of transects is presented in Fig. 1. Negative values indicate a southward flow.

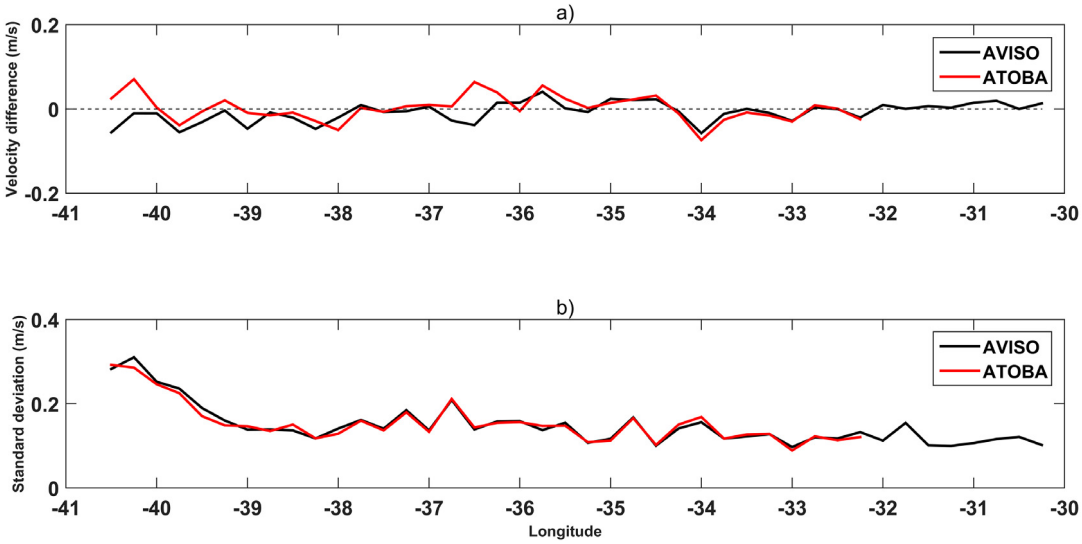


**Fig. 6.** Mean difference of velocity and standard deviation along the AX97 transect for AX97 and altimetry datasets (a and b, respectively). Positive velocity difference values indicate a more intense southward flow of AX97 when compared to altimetry dataset.

$-2.9 \pm 4.0$ Sv for AX97, $-6.1 \pm 7.5$ Sv for AVISO and $-5.3 \pm 8.2$ Sv for ATOBA datasets. Altimetry coupling resulted in a higher BC transport when compared to AX97. This result was expected for AVISO, once it tends to overestimate XBT based southward surface velocity along the AX97 transect. However, ATOBA also presented a considerable greater mean volume transport in comparison to AX97 (1.8 times greater than AX97 mean volume transport) (Fig. 8.a and 8.c), even though ATOBA surface velocities estimated northward AX97 surface velocities by only 3%. This could possibly be explained by the elevated rate of occurrence of opposite velocity vectors between altimetry products and AX97 data at the BC area of influence (>40%).

Fig. 9 shows the section of mean velocity across the AX97 transect for CP for all data used in this research and confirms the analysis above. ATOBA presents a shallow southward flow balanced by a subsurface equatorward flow that results in a neutral integrated transport down to the isopycnal of reference from 40.5° to 39.88°W (Figs. 8.c and 9.c). On the other hand, from 39.88° to 39°W, an intense southward flow was predominant on ATOBA dataset which resulted in a transport of $-5.3 \pm 8.2$ Sv. Nevertheless, all values achieved by the datasets analyzed were in agreement with the values reported by several authors (Signorini, 1978; Lima, 1997; Mata et al., 2012; Pereira et al., 2014; Lima et al., 2016). This fact should encourage other studies to continue the development of varied merging coupling methodologies, such as using ARGO data for referencing geostrophic velocity profiles.

### 3.2.1. Study cases

Cruises #7 and #20 (Table 1) were used as study cases based on their contrasting results. For the twentieth MOVAR cruise, the BC mean volume transport was estimated in $-3.2$ Sv for AX97, $-5.9$ Sv for AVISO and $-5.9$ Sv for ATOBA datasets (Fig. 10). As observed in the mean transport, the transport obtained by AX97 data was overestimated by both altimetry coupling methods. Fig. 11 presents the subsurface velocity structure along the AX97 reference transect during the 20th MOVAR cruise. All datasets

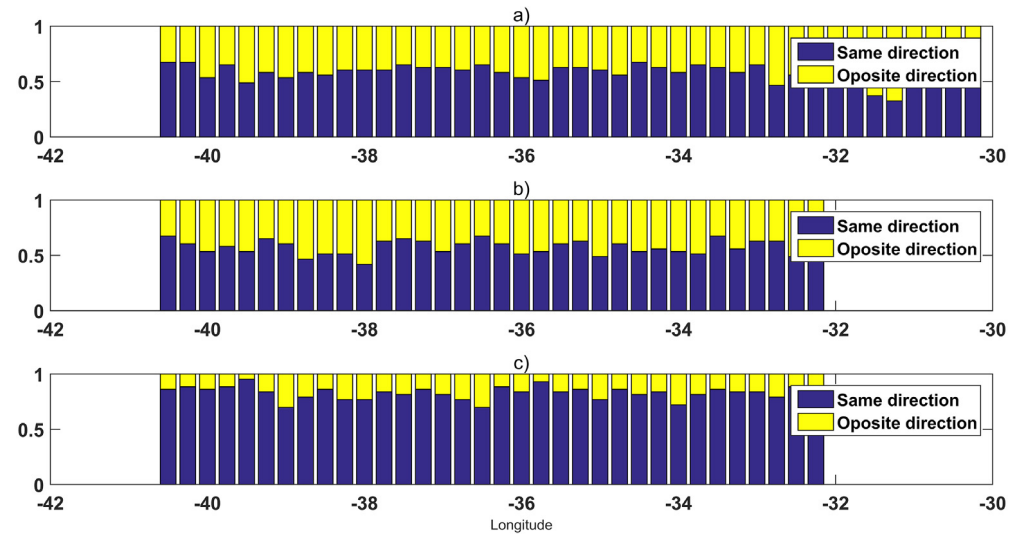


**Fig. 7.** Frequency of occurrence for altimetry and AX97 datasets at same and opposite directions along the AX97 transect (blue and yellow bars, respectively). Upper panel (a) represents the comparison between AX97 and AVISO datasets. Middle panel (b) shows the comparison between AX97 and ATOBA datasets. Lower panel (c) shows when both altimetry products agree/disagree on the direction at the same time. (For interpretation of the references to color in this figure legend, the reader is referred to the web version of this article.)

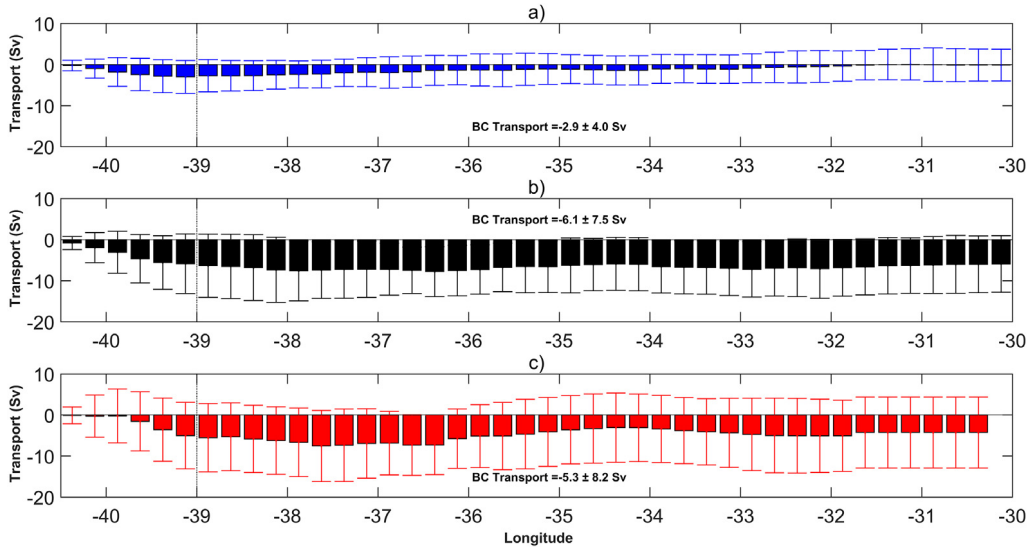


**Fig. 8.** Cumulative graphic of the mean integrated volume transport in Sv (from surface down to isopycnal of $\sigma_\Theta = 26.8$ kg/m$^3$) flowing across the AX97 transect during cruise periods assuming: (a) a level of no motion at the $\sigma_\theta = 26.8$ kg/m$^3$) and a known surface satellite velocity from (b) AVISO and (c) ATOBA. Vertical lines represent the standard deviation for each point where the value was estimated. Geographical location of the transect is presented in Fig. 1. Negative values indicate a southward transport.

obtained similar BC core velocities (−0.32 m/s, −0.28 m/s and 0.27 m/s for AX97, AVISO and ATOBA, respectively). In addition, little variation of the BC main core depth was observed. The BC core was 55 m below surface based on AX97 and AVISO data and 105 m for ATOBA dataset (Fig. 11). In this context, cruise #20 was a successful case of matching up altimetry and AX97 datasets.

However, aware of all error sources presented on the coupling methodology applied, Figs. 12 and 13 exemplify a case where the combination between AX97 and altimetry data resulted in non-realistic results (cruise #7). For this case, the BC mean transport was estimated in −8.0 Sv for AX97, −7.6 Sv for AVISO and a northward opposite transport of 0.5 Sv for ATOBA dataset (Fig. 12). AX97 captured a surface BC core with a velocity of 0.91 m/s while the merge with AVISO and ATOBA obtained maximum poleward velocities of 0.48 and 0.54 m/s (Fig. 13). On the other hand, altimetry coupling presented a persistent equatorward flow on the western boundary (0.47 m/s and 0.79 m/s for AVISO and ATOBA coupling, respectively). The 7th MOVAR cruise confirms the findings of the previous section, where the methodology applied to obtain the vertical structure of the velocity, considering altimetry data, is not efficient when opposite surface velocity vectors between altimetry and AX97 datasets occurs. In addition, the coupling performed with AVISO achieved a better result due to its spatial resolution. The fact that AVISO surface velocity data is smoother than ATOBA resulted in fewer changes in surface velocity direction.

Based on this section, the merge between AX97 and altimetry datasets presents some inconsistencies when surface currents are in opposite directions. Hence, as the difference observed at the surface will propagate along the water column, this method will result in an increase of intensity with depth instead of a decrease of flow towards the reference level adopted. Finally,

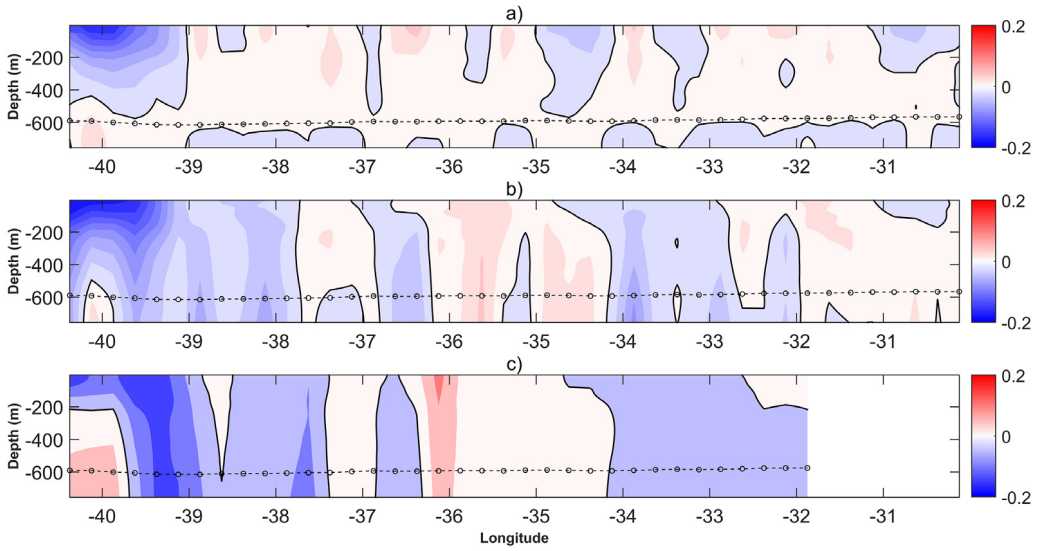


**Fig. 9.** Vertical distribution of the mean velocity across the AX97 transect for the cruise periods assuming: (a) a level of no motion at the $\sigma_\theta = 26.8$ kg/m$^3$ and a known surface satellite velocity from (b) AVISO and (c) ATOBA. The dashed line with open circles represents the mean depth of $\sigma_\theta = 26.8$ kg/m$^3$ isopycnal. Geographical location of the transect is presented in Fig. 1. Negative values indicate a southward flow.

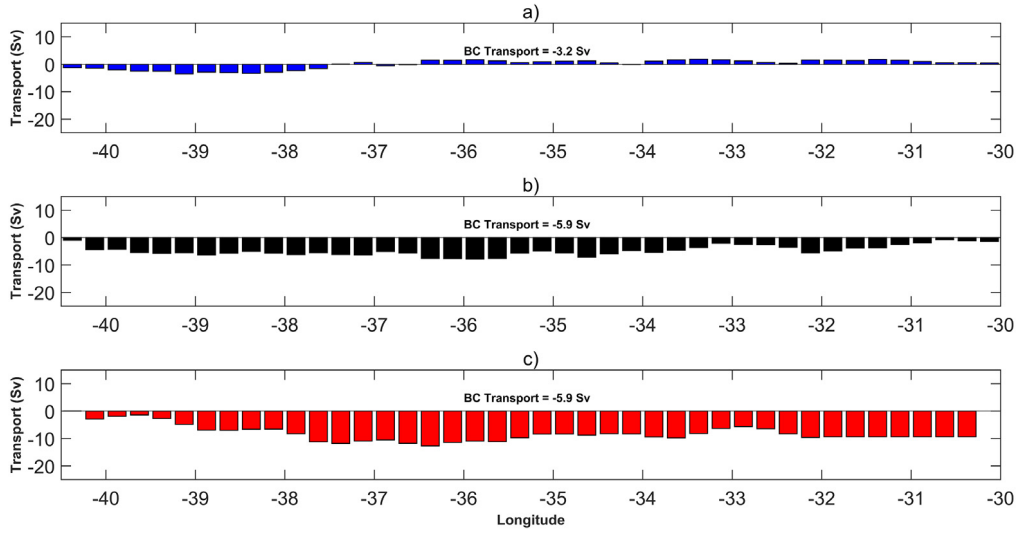


**Fig. 10.** Cumulative graphic of the integrated volume transport in Sv (from surface down to isopycnal of $\sigma_\theta = 26.8$ kg/m$^3$) flowing across the AX97 transect during 20th MOVAR cruise (Table 1) assuming: (a) a level of no motion at the $\sigma_\theta = 26.8$ kg/m$^3$ and a known surface satellite velocity from (b) AVISO and (c) ATOBA. Geographical location of the transect is presented in Fig. 1. Negative values indicate a southward transport.

as the methodology applied do not achieve a reliable outcome when combined data were in different directions, it is strongly recommended to use XBT data associated with deeper region data, where smaller intensity velocity will result on a propagation of a smaller error along water column.

## 4. Conclusion

An assessment of the influence of altimetry products, more specifically a high-resolution altimetry product (ATOBA), on improving the capabilities of dynamically analyzing the BC across the AX97 transect was performed. For that and based on in situ data, the BC eastern boundary was defined at 39°W. The impact of all limitations on the methodology applied was considered, but nevertheless data proved to be robust and representative both in terms of time and space.

The BC is an extremely variable feature and a high-resolution altimetry product could incorporate a significant amount of reliable data on its dynamical analysis. During the analyzed period, the BC was classified into three main stages, and the season with greater variability is the spring. Furthermore, ATOBA represented the surface horizontal BC velocities better than AVISO since this high-resolution altimetry product is more sensitive to the highly variable BC flow. The use of ATOBA dataset represents a gain of 3.4% on surface BC dynamical assessment when compared to AVISO, assuming MOVAR dataset as a reference. This improvement was partially caused by its higher resolution and partially caused by the use of coastal altimetry corrections on ATOBA product. The choice for coastal altimetry data was decisive on observing the BC core along the coastal areas where AX97 data was not acquired. However, on those areas, the bottom friction would increase its influence due to the proximity with the seabed and should be incorporated on the balance. Therefore, the assumption of geostrophic balance would not be valid and the balance between the pressure gradient force, Coriolis force and friction should be considered. In addition, the use of an isopycnal reference for AX97 data has certainly improved the

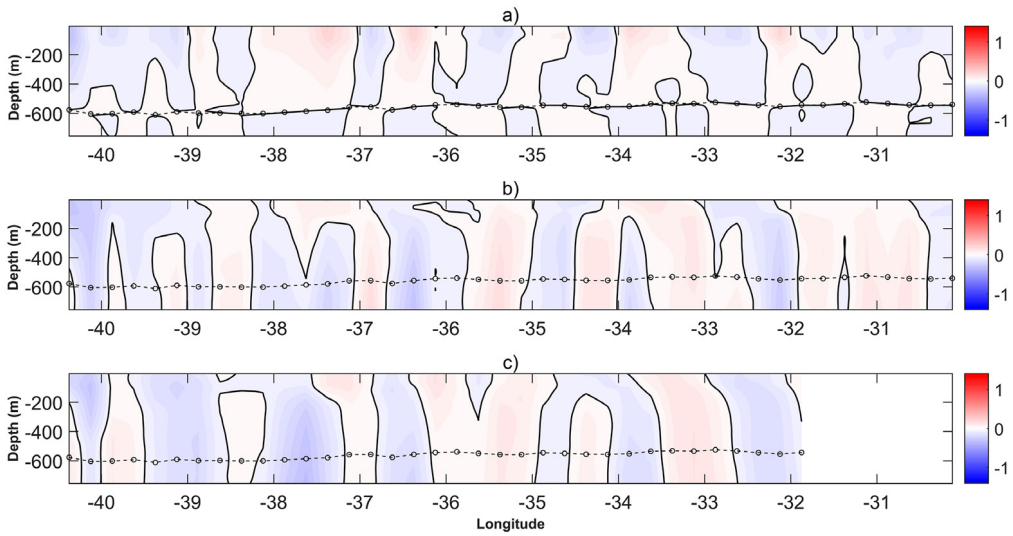


**Fig. 11.** Vertical distribution of the velocity across the AX97 transect during 20th MOVAR cruise (Table 1) assuming: (a) a level of no motion at the $\sigma_\theta = 26.8$ kg/m$^3$ and a known surface satellite velocity from (b) AVISO and (c) ATOB. The dashed line with open circles represents the depth of $\sigma_\theta = 26.8$ kg/m$^3$ isopycnal. Geographical location of the transect is presented in Fig. 1. Negative values indicate a southward flow.

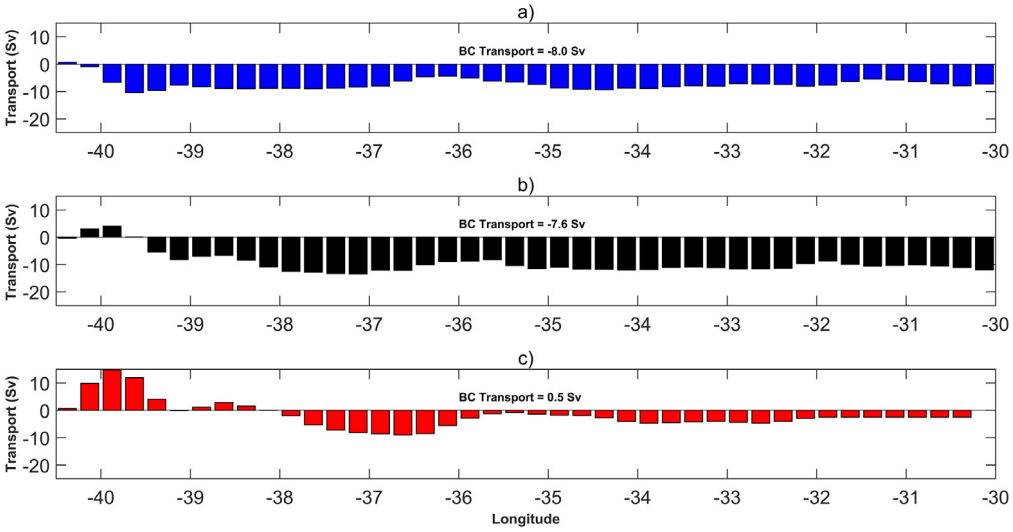


**Fig. 12.** Cumulative graphic of the integrated volume transport in Sv (from surface down to isopycnal of $\sigma_\theta = 26.8$ kg/m$^3$) flowing across the AX97 transect during 7th MOVAR cruise Table 1 assuming: (a) a level of no motion at the $\sigma_\theta = 26.8$ kg/m$^3$ and a known surface satellite velocity from (b) AVISO and (c) ATOBA. Geographical location of the transect is presented in Fig. 1. Negative values indicate a southward transport.

reliability of the results when compared to fixed reference depth levels adopted in previous studies (e.g. 400 m, 500 m), however, persistent efforts in determining precisely the reference level for geostrophic velocity estimation is strongly advised.

It is important to mention that when different products obtain different volume transport values for the same current in similar periods, it demonstrates the need of more independent measurements (e.g. surface drifters, shipborne ADCP) in order to claim a reference product. Therefore, more observational data surrounding AX97 region would be beneficial for the development of multiple reference products.

The use of high-resolution coastal altimetry to impose the surface velocity as the level of known velocity, in order to obtain the subsurface geostrophic currents based on XBT data, has shown that large discrepancies can arise when results are compared with the case where the reference level of zero velocity is at a given isopycnal level. For this strategy, we believe that the main source of errors arises from the fact that altimetry and XBT data incorporate different scales of time and space processes which may not be trivial to filter or isolate. Therefore, more efforts on the development of other methodologies for imposing the velocity at a certain reference level based on other types of in situ data is highly recommended. Considering that both the variability and the strength of the current itself reduces with depth, one promising possibility would be to derive this velocity based on a climatology of ARGO drifters at their parking depth (∼1000 m).

## Declaration of competing interest

The authors declare that they have no known competing financial interests or personal relationships that could have appeared to influence the work reported in this paper.

## Acknowledgments

The authors would like to thank the logistical support provided by the Brazilian Navy Hydrographic Office (DHN) and the Brazilian GOOS Program. XBT probes were provided by

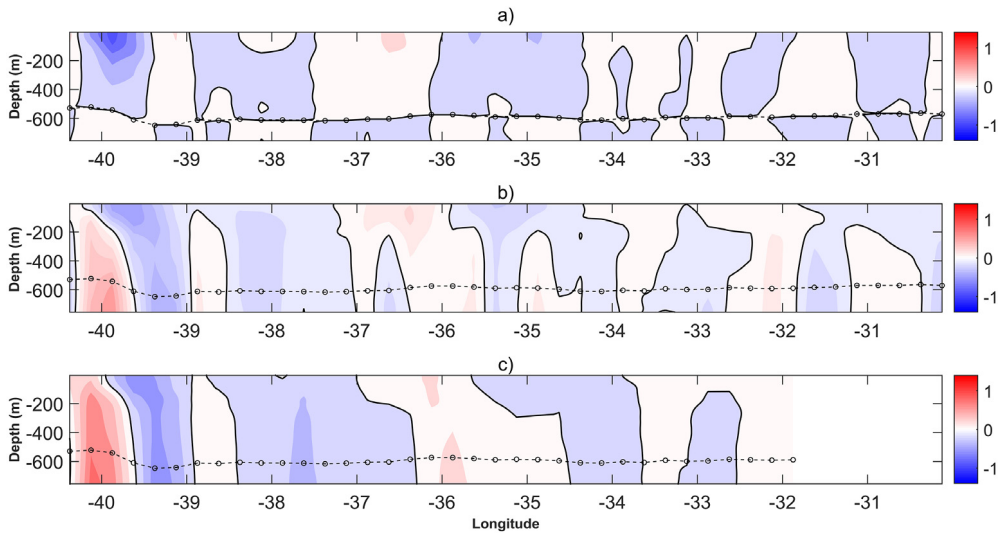


**Fig. 13.** Vertical distribution of the velocity across the AX97 transect during 7th MOVAR cruise (Table 1) assuming: (a) a level of no motion at the $\sigma_\theta = 26.8$ kg/m$^3$ and a known surface satellite velocity from (b) AVISO and (c) ATOBA. The dashed line with open circles represents the depth of $\sigma_\theta = 26.8$ kg/m$^3$ isopycnal. Geographical location of the transect is presented in Fig. 1. Negative values indicate a southward flow.

NOAA/AOML, funded by the NOAA Office of Climate Observations. Ivenis I. C. Pita, Mauro Cirano and Mauricio M. Mata were supported by Brazilian scholarships from the Brazilian National Council for Scientific and Technological Development (CNPq). This work was also partially funded by CNPq (405908/2016-4), Ministry of Science, Technology, Innovation and Communications (MCTIC), Brazil (01250.001271/2016-79) and from CAPES Foundation, Brazil (AUXPE 1995/2014). This research was supported by PETROBRAS and approved by the Brazilian oil regulatory agency ANP (Agência Nacional de Petróleo, Gás Natural e Biocombustíveis), under the special participation of Oceanographic Modeling and Observation Network (REMO) research project. The altimeter products (AVISO) were produced by Ssalto/Duacs and distributed by Aviso+, with support from Cnes (http://www.aviso.altimetry.fr/duacs/). The altimeter products (ATOBA) were produced by Ssalto/Duacs and distributed by the Oceanographic Modeling and Observation Network (REMO).

## References

Abraham, J.P., Baringer, M., Bindoff, N.L., Boyer, T., Cheng, L.J., Church, J.A., Conroy, J.L., Domingues, C.M., Fasullo, J.T., Gilson, J., Goni, G., Good, S.A., Gorman, J.M., Gouretski, V., Ishii, M., Johnson, G.C., Kizu, S., Lyman, J.M., Macdonald, A.M., Minkowycz, W.J., Moffitt, S.E., Palmer, M.D., Piola, A.R., Reseghetti, F., Schuckmann, K., Trenberth, K.E., Velicogna, I., Willis, J.K., 2013. A review of global ocean temperature observations: Implications for ocean heat content estimates and climate change. Rev. Geophys. 51, 450–483. http://dx.doi.org/10.1002/rog.20022.

Arruda, W.Z., Campos, E.J.D., Zharkov, V., Soutelino, R.G., da Silveira, I.C.A., 2013. Events of equatorward translation of the Vitoria Eddy. Cont. Shelf Res. 70, 61–73. http://dx.doi.org/10.1016/J.CSR.2013.05.004.

Benny, N.P., Mridula, K.R., Mahmud, M.R., Ses, S., Omar, K.M., 2015. Northern south China sea surface circulation and its variability derived by combining satellite altimetry and surface drifter data. Terr. Atmos. Ocean. Sci. 26, 193–203. http://dx.doi.org/10.3319/TAO.2014.12.02.04(EOSI).

Biló, T.C., da Silveira, I.C.A., Belo, W.C., de Castro, B.M., Piola, A.R., 2014. Methods for estimating the velocities of the Brazil Current in the pre-salt reservoir area off southeast Brazil (23°S–26°S). Ocean Dyn. 64, 1431–1446. http://dx.doi.org/10.1007/s10236-014-0761-2.

Birol, F., Fuller, N., Lyart, F., Cancet, M., Niño, F., Delebecque, C., Fleury, S., Toublanc, F., Melet, A., Saraceno, M., Léger, F., 2017. Coastal application from nadir altimetry: Example of the X-TRACK regional products. Adv. Space Res. 59, 936–953. http://dx.doi.org/10.1016/j.asr.2016.11.005.

Bringas, F., Goni, G., 2015. Early dynamics of deep blue XBT probes. J. Atmos. Ocean. Technol. 32, 2253–2263. http://dx.doi.org/10.1175/JTECH-D-15-0048.1.

Calado, L., Gangopadhyay, A., da Silveira, I.C.A., 2008. Feature-oriented regional modeling and simulations (FORMS) for the western South Atlantic: Southeastern Brazil region. J. Ocean Modelling 25, 48–64. http://dx.doi.org/10.1016/j.ocemod.2008.06.007.

Campos, E.J.D., 2006. Equatorward translation of the Vitoria Eddy in a numerical simulation. Geophys. Res. Lett. 33, L22607. http://dx.doi.org/10.1029/2006GL026997.

Campos, E.J.D., Gonçalves, J.E., Ikeda, Y., 1995. Water mass characteristics and geostrophic circulation in the South Brazil Bight: Summer of 1991. J. Geophys. Res. 100, 18537. http://dx.doi.org/10.1029/95JC01724.

Chelton, D., Ries, J., Haines, B., Fu, L., Callahan, P., 2001. In: Fu, L., Cazenave, A. (Eds.), Satellite altimetry, in Satellite Altimetry and Earth Sciences: A Handbook of Techniques and Applications. In: International Geophysics, pp. 1–131.

Cheng, L., Abraham, J., Goni, G., Boyer, T., Wijffels, S., Cowley, R., Gouretski, V., Reseghetti, F., Kizu, S., Dong, S., Bringas, F., Goes, M., Houpert, L., Sprintall, J., Zhu, J., 2016. XBT science: Assessment of instrumental biases and errors. Bull. Am. Meteorol. Soc. 97, 923–933. http://dx.doi.org/10.1175/BAMS-D-15-00031.1.

Cheng, L., Zhu, J., Cowley, R., Boyer, T., Wijffels, S., 2014. Time, probe type, and temperature variable bias corrections to historical expendable bathythermograph observations. J. Atmos. Ocean. Technol. 31, 1793–1825. http://dx.doi.org/10.1175/JTECH-D-13-00197.1.

CLS, 2015a. SSALTO/DUACS User Handbook: (M)SLA and (M)ADT Near-Real Time and Delayed Time Products, CLS-DOS-NT-06-034.

CLS, 2015b. SSALTO/DUACS User Handbook: Regional Brazilian Altimetry products (ATOBA), CLS-DOS-NT-2013-242.

da Silveira, I.C.A., Calado, L., Castro, B.M., Cirano, M., Lima, J.A.M., Mascarenhas, A.d.S., 2004. On the baroclinic structure of the Brazil Current-Intermediate Western Boundary Current system at 22°-3°S. Geophys. Res. Lett. 31, L14308. http://dx.doi.org/10.1029/2004GL020036.

da Silveira, I.C.A., Lima, J.A.M., Schmidt, A.C.K., Ceccopieri, W., Sartori, A., Francisco, C.P.F., Fontes, R.F.C., 2008. Is the meander growth in the Brazil Current system off Southeast Brazil due to baroclinic instability? Dyn. Atmos. Ocean. 45, 187–207. http://dx.doi.org/10.1016/j.dynatmoce.2008.01.002.

Daher, V.B., Junior, P.R.C., 2014. Produto altimétrico regional para a área de interesse da Rede Temática de Modelagem e Observação Oceanográfica ( REMO ). Rev. Pesqui. Nav. 26, 22–33.

DiNezio, P.N., Goni, G.J., 2010. Identifying and estimating biases between XBT and Argo observations using satellite altimetry. J. Atmos. Ocean. Technol. 27, 226–240. http://dx.doi.org/10.1175/2009JTECHO711.1.

DiNezio, P.N., Goni, G.J., 2011. Direct evidence of a changing fall-rate bias in XBTs manufactured during 1986-2008. J. Atmos. Ocean. Technol. 28, 1569–1578. http://dx.doi.org/10.1175/JTECH-D-11-00017.1.

Ding, R., Huang, D., Xuan, J., Mayer, B., Zhou, F., Pohlmann, T., 2016. Cross-shelf water exchange in the East China Sea as estimated by satellite altimetry and in situ hydrographic measurement. J. Geophys. Res. Ocean 121, 7192–7211. http://dx.doi.org/10.1002/2016JC011972.

Dong, S., Garzoli, S., Baringer, M., Meinen, C., Goni, G., 2009. Interannual variations in the Atlantic meridional overturning circulation and its relationship with the net northward heat transport in the South Atlantic. Geophys. Res. Lett. 36, L20606. http://dx.doi.org/10.1029/2009GL039356.

Dong, S., Goni, G., Bringas, F., 2015. Temporal variability of the South Atlantic meridional overturning circulation between 20°S and 35°S. Geophys. Res. Lett. 42, 7655–7662. http://dx.doi.org/10.1002/2015GL065603.

Dufau, C., Martin-Puig, C., Moreno, L., 2011. User requirements in the coastal ocean for satellite altimetry. In: Coastal Altimetry. Springer Berlin Heidelberg, Berlin, Heidelberg, pp. 51–60. http://dx.doi.org/10.1007/978-3-642-12796-0_3.

Evans, D.L., Signorini, S.S., 1985. Vertical structure of the Brazil Current. Nature 315, 48–50. http://dx.doi.org/10.1038/315048a0.

Evans, D.L., Signorini, S.R., Miranda, L.B., 1983. A note on the transport of the Brazil Current. J. Phys. Oceanogr. 13, 1732–1738. http://dx.doi.org/10.1175/1520-0485(1983)013<1732:ANOTTO>2.0.CO;2.

Fu, L.-L., 1981. The general circulation and meridional heat transport of the subtropical South Atlantic determined by inverse methods. J. Phys. Oceanogr. 11, 1171–1193. http://dx.doi.org/10.1175/1520-0485(1981)011<1171:TGCAMH>2.0.CO;2.

García, P., Martin-Puig, C., Roca, M., 2018. SARin mode, and a window delay approach, for coastal altimetry. Adv. Space Res. 62, 1358–1370. http://dx.doi.org/10.1016/j.asr.2018.03.315.

Garzoli, S.L., Baringer, M.O., 2007. Meridional heat transport determined with expandable bathythermographs-Part II: South Atlantic transport. Deep-Sea Res. I 54, 1402–1420. http://dx.doi.org/10.1016/j.dsr.2007.04.013.

Goes, M., Baringer, M., Goni, G., 2015a. The impact of historical biases on the XBT-derived meridional overturning circulation estimates at 34°S. Geophys. Res. Lett. 42, 1848–1855. http://dx.doi.org/10.1002/2014GL061802.

Goes, M., Goni, G., Dong, S., 2015b. An optimal XBT-based monitoring system for the South Atlantic meridional overturning circulation at 34°S. J. Geophys. Res. Ocean 120, 161–181. http://dx.doi.org/10.1002/2014JC010202.

Goes, M., Goni, G., Hormann, V., Perez, R.C., 2013a. Variability of the Atlantic off-equatorial eastward currents during 1993-2010 using a synthetic method. J. Geophys. Res. Ocean 118, 3026–3045. http://dx.doi.org/10.1002/jgrc.20186.

Goes, M., Goni, G., Keller, K., 2013b. Reducing biases in XBT measurements by including discrete information from pressure switches. J. Atmos. Ocean. Technol. 30, 810–824. http://dx.doi.org/10.1175/JTECH-D-12-00126.1.

Harris, P.T., Tsuji, Y., Marshall, J.F., Davies, P.J., Honda, N., Matsuda, H., 1996. Sand and rhodolith-gravel entrainment on the mid- to outer-shelf under a western boundary current: Fraser Island continental shelf, eastern Australia. Mar. Geol. 129, 313–330. http://dx.doi.org/10.1016/0025-3227(96)83350-0.

Hutchinson, K.A., Swart, S., Ansorge, I.J., Goni, G.J., 2013. Exposing XBT bias in the Atlantic sector of the Southern Ocean. Deep-Sea Res. I 80, 11–22. http://dx.doi.org/10.1016/j.dsr.2013.06.001.

Huthnance, J.M., 1995. Circulation, exchange and water masses at the ocean margin: the role of physical processes at the shelf edge. Prog. Oceanogr. 35, 353–431. http://dx.doi.org/10.1016/0079-6611(95)80003-C.

Laurindo, L.C., Mariano, A.J., Lumpkin, R., 2017. An improved near-surface velocity climatology for the global ocean from drifter observations. Deep-Sea Res. I 124, 73–92. http://dx.doi.org/10.1016/j.dsr.2017.04.009.

Legeais, J.F., Ollitrault, M., Arhan, M., 2013. Lagrangian observations in the intermediate western boundary current of the South Atlantic. Deep-Sea Res. II 85, 109–126. http://dx.doi.org/10.1016/j.dsr2.2012.07.028.

Lima, J.A.M., 1997. Oceanic Circulation on the Brazilian Shelf Break and Slope at 22°S (Ph.D. thesis). UNSW. Kensington, N.S.W, Australia, p. 164.

Lima, M.O., Cirano, M., Mata, M.M., Goes, M., Goni, G., Baringer, M., 2016. An assessment of the Brazil Current baroclinic structure and variability near 22°s in Distinct Ocean Forecasting and Analysis Systems. Ocean Dyn. 66, 893–916. http://dx.doi.org/10.1007/s10236-016-0959-6.

Lutjeharms, J.R.E., Catzel, R., Valentine, H.R., 1989. Eddies and other boundary phenomena of the Agulhas Current. Cont. Shelf Res. 9, 597–616. http://dx.doi.org/10.1016/0278-4343(89)90032-0.

Mascarenhas, A., Miranda, B., Rock, Y., 1971. A study of the oceanographic conditions in the region of Cabo Frio. Fertil. Sea 1, 285–308.

Mata, M.M., Cirano, M., van Caspel, M.R., Fonteles, C.S., Goñi, G., Beringer, M., 2012. Observations of the Brazil Current baroclinic transport near 22°S: variability from the AX97 XBT transect. Clivar Exch. 17, 5–10.

Mill, G.N., da Costa, V.S., Lima, N.D., Gabioux, M., Guerra, L.A.A., Paiva, A.M., 2015. Northward migration of Cape São Tomé rings, Brazil. Cont. Shelf Res. 106, 27–37. http://dx.doi.org/10.1016/j.csr.2015.06.010.

Müller, T.J., Ikeda, Y., Zangenberg, N., Nonato, L.V., 1998. Direct measurements of western boundary currents off Brazil between 20°S and 28°S. J. Geophys. Res. Ocean 103, 5429–5437. http://dx.doi.org/10.1029/97JC03529.

Palóczy, A., da Silveira, I.C.A., Castro, B.M., Calado, L., 2014. Coastal upwelling off Cape São Tomé (22°S, Brazil): The supporting role of deep ocean processes. Cont. Shelf Res. 89, 38–50. http://dx.doi.org/10.1016/J.CSR.2013.09.005.

Passaro, M., Cipollini, P., Vignudelli, S., Quartly, G.D., Snaith, H.M., 2014. ALES: A multi-mission adaptive subwaveform retracker for coastal and open ocean altimetry. Remote Sens. Environ. 145, 173–189. http://dx.doi.org/10.1016/j.rse.2014.02.008.

Passaro, M., Rose, S.K., Andersen, O.B., Boergens, E., Calafat, F.M., Dettmering, D., Benveniste, J., 2018. ALES+: Adapting a homogenous ocean retracker for satellite altimetry to sea ice leads, coastal and inland waters. Remote Sens. Environ. 211, 456–471. http://dx.doi.org/10.1016/j.rse.2018.02.074.

Pereira, J., Gabioux, M., Marta-Almeida, M., Cirano, M., Paiva, A.M., Aguiar, A.L., 2014. The bifurcation of the western boundary current system of the South Atlantic Ocean. Rev. Bras. Geofís. 32, 241–257. http://dx.doi.org/10.22564/rbgf.vol32n2-2014.

Pond, S., Pickard, G.L., 1983. Currents without friction: Geostrophic flow. In: Introductory Dynamical Oceanography. Elsevier, pp. 63–99. http://dx.doi.org/10.1016/B978-0-08-057054-9.50014-6.

Reverdin, G., Marin, F., Bourlès, B., L'Herminier, P., 2009. XBT temperature errors during french research cruises (1999-2007). J. Atmos. Ocean. Technol. 26, 2462–2473. http://dx.doi.org/10.1175/2009JTECHO655.1.

Ribeiro, N., Mata, M., de Azevedo, J., Cirano, M., 2018. An assessment of the XBT fall-rate equation in the Southern Ocean. J. Atmos. Ocean. Technol. 35, 911–926. http://dx.doi.org/10.1174/JTECH-D-17-0086.1.

Roblou, L., Lamouroux, J., Bouffard, J., Lyard, F., Le Hénaff, M., Lombard, A., Marsaleix, P., De Mey, P., Birol, F., 2011. Post-processing altimeter data towards coastal applications and integration into coastal models. In: Coastal Altimetry. Springer Berlin Heidelberg, Berlin, Heidelberg, pp. 217–246. http://dx.doi.org/10.1007/978-3-642-12796-0_9.

Rocha, C.B., Da Silveira, I.C.A., Castro, B.M., Lima, J.A.M., 2014. Vertical structure, energetics, and dynamics of the Brazil Current System at 22°S-28°S. J. Geophys. Res. Ocean 119, 52–69. http://dx.doi.org/10.1002/2013JC009143.

Savidge, D.K., Bane, J.M., 2001. Wind and Gulf Stream influences on along-shelf transport and off-shelf export at Cape Hatteras, North Carolina. J. Geophys. Res. Ocean 106, 11505–11527. http://dx.doi.org/10.1029/2000JC000574.

Schaeffer, A., Roughan, M., Wood, J.E., 2014. Observed bottom boundary layer transport and uplift on the continental shelf adjacent to a western boundary current. J. Geophys. Res. Ocean 119, 4922–4939. http://dx.doi.org/10.1002/2013JC009735.

Schmid, C., Schäfer, H., Zenk, W., Podestá, G., 1995. The Vitória Eddy and its relation to the Brazil Current. J. Phys. Oceanogr. 25, 2532–2546. http://dx.doi.org/10.1175/1520-0485(1995)025<2532:TVEAIR>2.0.CO;2.

Signorini, S.R., 1978. On the circulation and the volume transport of the Brazil Current between the Cape of São Tomé and Guanabara Bay. Deep. Res. 25, 481–490. http://dx.doi.org/10.1016/0146-6291(78)90556-8.

Simpson, J.H., Sharples, J., 2012. Introduction to the Physical and Biological Oceanography of Shelf Seas. http://dx.doi.org/10.1017/CBO9781139034098.

Soutelino, R.G., Da Silveira, I.C.A., Gangopadhyay, A., Miranda, J.A., 2011. Is the Brazil Current eddy-dominated to the north of 20°S? Geophys. Res. Lett. 38, L03607. http://dx.doi.org/10.1029/2010GL046276.

Sprintall, J., Wijffels, S., Chereskin, T., Bray, N., 2002. The JADE and WOCE I10/IR6 throughflow sections in the southeast Indian Ocean. Part 2: velocity and transports. Deep-Sea Res. II 49, 1363–1389. http://dx.doi.org/10.1016/S0967-0645(01)00163-1.

Stramma, L., England, M., 1999. On the water masses and mean circulation of the South Atlantic Ocean. J. Geophys. Res. Ocean 104, 20863–20883. http://dx.doi.org/10.1029/1999JC900139.

Stramma, L., Ikeda, Y., Peterson, R.G., 1990. Geostrophic transport in the Brazil current region north of 20°S. Deep-Sea Res. A 37, 1875–1886. http://dx.doi.org/10.1016/0198-0149(90)90083-8.

Thacker, W.C., 2007. Estimating salinity to complement observed temperature: 1. Gulf of Mexico. J. Mar. Syst. 65, 224–248. http://dx.doi.org/10.1016/J.JMARSYS.2005.06.008.

Thacker, W.C., Sindlinger, L., 2007. Estimating salinity to complement observed temperature: 2. Northwestern Atlantic. J. Mar. Syst. 65, 249–267. http://dx.doi.org/10.1016/J.JMARSYS.2005.06.007.

van Caspel, M.R., Mata, M.M., Cirano, M., 2010. Sobre a relação TS na porção central do Atlântico Sudoeste: uma contribuição para o estudo da variabilidade oceânica no entorno da Cadeia Vitória-Trindade [About TS relationship in the central portion of the Southwestern Atlantic: a contribution to the study of the oceanic variability surrounding Vitória-Trindade Ridge]. Atlantica 32 (1), 95–110. http://dx.doi.org/10.5088/atl.2010.32.1.95.